Front. Energy 2023, 17(5): 678–691
https://doi.org/10.1007/s11708-022-0859-z

RESEARCH ARTICLE

**Haoqing WU, Yaoyuan ZHANG, Shijie MI, Wenbin ZHAO, Zhuoyao HE, Yong QIAN, Xingcai LU**

# A methodology for regulating fuel stratification and improving fuel economy of GCI mode via double main-injection strategy



**Abstract** Gasoline compression ignition (GCI) combustion faces problems such as high maximum pressure rise rate (MPRR) and combustion deterioration at high loads. This paper aims to improve the engine performance of the GCI mode by regulating concentration stratification and promoting fuel-gas mixing by utilizing the double main-injection (DMI) strategy. Two direct injectors simultaneously injected gasoline with an octane number of 82.7 to investigate the energy ratio between the two main-injection and exhaust gas recirculation (EGR) on combustion and emissions. High-load experiments were conducted using the DMI strategy and compared with the single main-injection (SMI) strategy and conventional diesel combustion. The results indicate that the DMI strategy have a great potential to reduce the MPRR and improve the fuel economy of the GCI mode. At a 10 bar indicated mean effective pressure, increasing the main-injection-2 ratio ($R_{\mathrm{m}\text{-}2}$) shortens the injection duration and increases the mean mixing time. Optimized $R_{\mathrm{m}\text{-}2}$ could moderate the trade-off between the MPRR and the indicated specific fuel consumption with both reductions. An appropriate EGR should be adopted considering combustion and emissions. The DMI strategy achieves a highly efficient and stable combustion at high loads, with an indicated thermal efficiency (ITE) greater than 48%, CO and THC emissions at low levels, and MPRR within a reasonable range. Compared with the SMI strategy, the maximum improvement of the ITE is 1.5%, and the maximum reduction of MPRR is 1.5 bar/°CA.

**Keywords** gasoline compression ignition, injection strategy, fuel stratification, high efficiency, high load

Received Aug. 1, 2022; accepted Nov. 20, 2022; online Jan. 10, 2023

Haoqing WU, Yaoyuan ZHANG, Shijie MI, Wenbin ZHAO, Zhuoyao HE, Yong QIAN (✉), Xingcai LU
Key Laboratory for Power Machinery and Engineering of the Ministry of Education, Shanghai Jiao Tong University, Shanghai 200240, China
E-mail: qiany@sjtu.edu.cn

## 1 Introduction

Exploring advanced combustion mode with high efficiency and low emissions has been the dream of successive generations of researchers [1,2]. Conventional diesel engines have high compression ratios thus with thermal efficiencies of 35%–45%, but the diffusion combustion characteristics of diesel make $NO_x$ and soot emissions high. The gasoline engine has a homogeneous fuel-gas mixture before combustion thus with low $NO_x$ and soot emissions, but the low compression ratio results in a thermal efficiency of gasoline engines between 30% and 35%. Gasoline compression ignition (GCI) is an advanced combustion mode in the field of internal combustion engines, which combines the advantages of the high efficiency of diesel engines and the low emissions of gasoline engines. The GCI mode was proposed by Kalghatgi and Ångström [3], who creatively applied gasoline to compression ignition engines. Because of the high compression ratio and small pumping losses of compression ignition engines as well as the high volatility and low reactivity of gasoline, the gas mixture was highly diluted before ignition [4]. Therefore, the GCI mode can achieve a higher thermal efficiency than gasoline engines and lower emissions than diesel engines. Subsequently, many researchers conducted studies on the GCI mode [5,6].

Hanson et al. [7] conducted experiments on a heavy-duty compression ignition engine using the 91 pump octane number gasoline. The results showed that the two injections in the compression stroke in combination with the 20% exhaust gas recirculation (EGR) ensured low $NO_x$ and PM emissions while achieving an indicated thermal efficiency of about 47% at a 11 bar indicated mean effective pressure (IMEP). Kim et al. [8] compared the spray and combustion of gasoline and diesel. The results showed that gasoline spray exhibited a shorter penetration length and a narrower spray angle than diesel spray under evaporation conditions, and gasoline combustion had a lower soot emission than diesel combustion. Ciatti and Subramanian [9] investigated the effects of injection strategy, EGR, and injection pressure on combustion and emissions using 84 research octane number gasoline. The results indicated that gasoline operation had a comparable fuel efficiency with a lower $NO_x$ emission than conventional diesel combustion, and the brake thermal efficiency (BTE) of gasoline combustion reached about 37% at a 12 bar brake mean effective pressure. Kalghatgi et al. [10] successfully used gasoline on a multi-cylinder diesel engine without making any changes. The results indicated that compared to diesel fuel with similar $NO_x$ levels, gasoline allowed engine operation with a lower smoke, a lower maximum pressure rise rate (MPRR), and a lower brake specific fuel consumption but with higher CO and THC emissions, and the BTE could reach about 39% at 10 bar IMEP. Delphi Corporation [11] had upgraded the GDCI engine for three iterations. The third generation of the engine brought its BTE to 43.5%. All of these indicate that the GCI mode has a practical application potential.

Although the GCI mode can achieve a high efficiency while maintaining low $NO_x$ and soot emissions, the load range of such high efficiency and low emissions is finite. The problems of high MPRR, combustion deterioration at high loads, and combustion instability at low loads still need to be solved [12,13]. Thereinto, it is particularly urgent to solve the problems at high loads, because it affects the dynamics of the engine. At high loads, the increase in the fuel injection amount leads to a longer injection duration, resulting in a shorter fuel-gas mixing time. Although increasing the nozzle hole diameter could increase the fuel injection amount per unit time and shorten the injection duration, the spray quality became poor, resulting in a lower fuel efficiency and higher soot emissions [14]. Increasing the injection pressure could reduce the injection duration and improve the spray quality. However, many researchers believed that it is difficult for the fuel injection system to maintain a high injection pressure at high loads due to the cavitation, airlock, and internal leakage caused by the low viscosity of gasoline [15,16]. In addition, increasing the injection pressure increases the amount of combustible mixture, causing multiple points of ignition and thus significantly increasing the MPRR. Moreover, the high injection pressure would exacerbate the combustion instability of the GCI mode at low loads due to the low in-cylinder reactivity. Ultimately, single-injector injection at large fuel demand cannot achieve a rapid fuel supply and form a reasonable concentration stratification before ignition, thus resulting in combustion deterioration and a high MPRR. Furthermore, the single-injector injection cannot balance the fuel demand between low and high loads.

Some researchers adopted the multi-stage injection strategy to inject fuel into the cylinder to shorten the main injection duration. However, the early injection of fuel into the cylinder increased CO and THC emissions due to the wall wetting problem, resulting in the deterioration of combustion efficiency [17]. Jiang et al. [18] shortened the direct injection duration at high loads by adding a port injector to share the direct injection fuel. The direct injection in combination with the port injection reduced combustion noise and particulate matter emissions, but CO and THC emissions were high and the thermal efficiency would be lower than that of the direct injection strategy due to insufficient oxidation. In the area of aero-engines and marine engines, two and more injectors were installed on each cylinder to achieve a good fuel atomization and combustion to alleviate the lack of injection pressure and shorten the injection duration [19,20].

Motivated by the applications of multiple injectors on aero-engines and marine engines, this paper proposes a new methodology to achieve rapid fuel supply. Two direct injectors are used for the simultaneous main-injection near the top dead center, called the double main-injection (DMI) strategy, which can alleviate the requirement for high injection pressure of the GCI mode and achieve a good fuel-gas mixing. The injection mass ratio between the two main-injections can be adjusted to regulate the in-cylinder concentration stratification, thus achieving a controlled combustion. In addition, the near-top-dead-center injection of the two injectors can ease the wall wetting problem, which reduces incomplete combustion emissions. Moreover, two injectors allow for a balance of large and small load injection demands.

As discussed above, the GCI mode faces problems such as combustion deterioration and a high MPRR at high loads. Therefore, experiments were performed on a modified single-cylinder engine with two independent direct injection systems. The main purpose of this study is to explore the effect of the DMI strategy on the combustion and emissions of the GCI mode and further achieve a highly efficient and stable operation of the GCI mode at high loads using the DMI strategy. The effects of the main-injection-2 ratio ($R_{m\text{-}2}$) and EGR on the combustion and emissions were first systematically investigated. Then, high-load experiments were conducted using the DMI strategy and compared with the single main-injection (SMI) strategy to reveal the advantages of the DMI strategy in regulating concentration stratification and improving fuel economy. The findings of this study are an important guide for the efficient and stable operation of the GCI mode.

## 2 Experimental methods

### 2.1 Engine and instrumentations

Experiments were conducted on a four-cylinder turbocharged DI diesel engine that met the Euro 5 emission standards. The fourth cylinder was modified into the tested cylinder which had an independent intake and exhaust system, while an additional direct injection injector was installed on the cylinder head. The two sets of direct injection systems, the original injector (injector 1) and the newly installed injector (injector 2), could independently adjust the injection timing and the injection pulse width and were driven by additional outside power systems. The newly installed injector was almost symmetrically placed with the original injector. The supercharger was powered by an outside power system to supply the charged air to the tested cylinder. The other three cylinders still operated in the original working mode. Table 1 lists the main parameters of the engine.

In-cylinder pressure was recorded by a cylinder pressure sensor (Kistler 6115B) with a sampling interval of 0.5 °CA and 100 in-cylinder pressure cycles. The recorded cylinder pressure signal was transmitted to a D2T Orisis combustion analyzer via a charge amplifier (Kistler model 5015A) to calculate the combustion parameters such as the maximum pressure rise rate (MPRR), CA10, CA50, and CA90 parameters. CA10, CA50, and CA90 were defined as the crank angle for 10%, 50%, and 90% of the total heat release, respectively.

**Table 1** Test engine specifications

| Parameters | Value |
|---|---|
| Stroke/mm | 130 |
| Bore/mm | 114 |
| Conrod length/mm | 216 |
| Number of strokes | 4 |
| Displacement(single)/L | 1.325 |
| Compression ratio | 18:1 |
| Intake valve open/(°CA ATDC) | 338 |
| Intake valve close/(°CA BTDC) | 145 |
| Exhaust valve open/(°CA ATDC) | 112 |
| Exhaust valve close/(°CA BTDC) | 335 |

Gaseous pollutant emissions were measured using a high-resolution Fourier transform infra-red (FTIR) gas analyzer with a sampling frequency of 5 Hz. The particle size distribution and the total number of particles were continuously measured by the DMS500 fast particulate analyzer produced with a measurement range of 5–1000 nm and a response time of 200 ms. To ensure the accuracy and reliability of all test results, each sample point was recorded for one minute after the engine had been operated steadily for three minutes. Figure 1 is a schematic diagram of the structure of the test cylinder.

### 2.2 Fuels

Extensive experimental results showed that the low-octane gasoline could be successfully used in compression ignition engines and exhibited good combustion and emission characteristics [21–23]. In addition, a process-based, well-to-wheel conceptualized life cycle assessment model showed that the low-octane gasoline-GCI pathway led to a 24.6% reduction in energy consumption and a 22.8% reduction in greenhouse gas emissions compared with the conventional pathway [24]. Kalghatgi et al. [23] believed that gasoline with octane numbers between 75

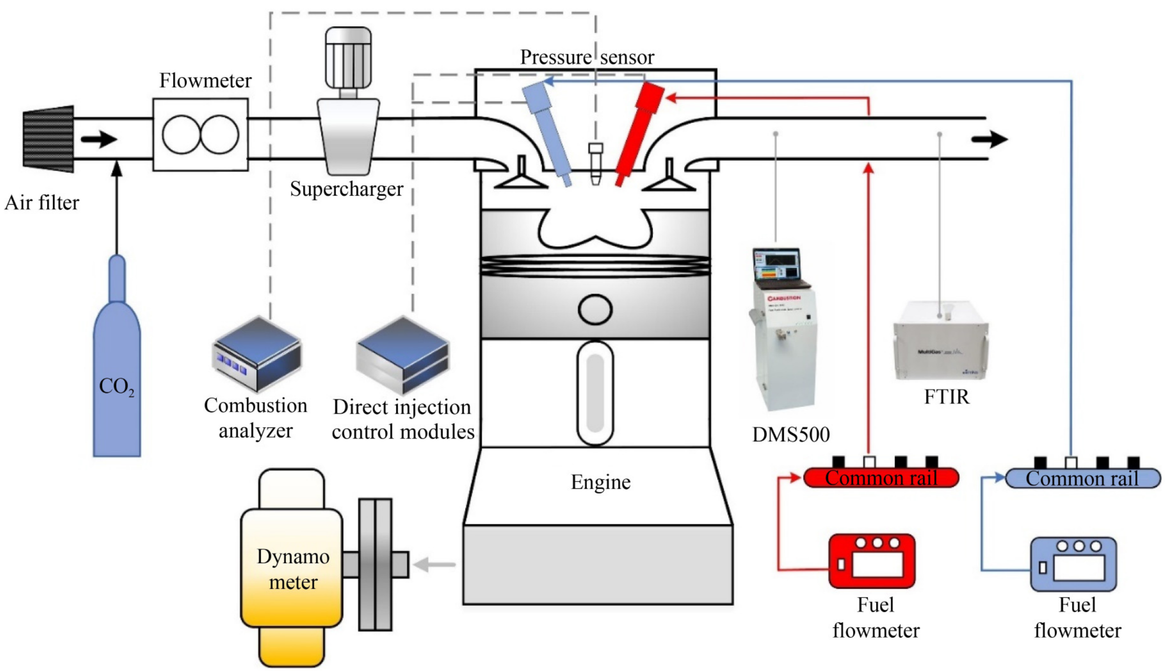


**Fig. 1** Schematic of experimental setup.

and 85 was more suitable for the GCI mode. Therefore, the gasoline supplied by Shandong Chambroad Petrochemicals Ltd. with a research octane number (RON) of 82.7, denoted as G80, was selected for the GCI experiments in this study. Additionally, to protect the fuel injection system from excessive wear and increase the viscosity of the fuel, $2 \times 10^{-4}$ (v/v) additives were added to the fuel without affecting other fuel properties. No. 0 diesel that met the CHINA VI standard was used for the CDC mode test. The fuel properties are listed in Table 2.

### 2.3 Test conditions

In previous studies, the main injection strategy demonstrated a better thermal efficiency than the pre-injection plus main injection strategy and low regulated emissions [18,22]. Therefore, two direct injectors were used for the main-injection near the top dead center, called the double main-injection (DMI) strategy, to achieve a rapid fuel supply for fuel-gas mixing. The main-injection time of the two injectors was kept consistent. In addition, the single main-injection (SMI) strategy and conventional diesel combustion were performed with injector 1 as a comparison to fully understand the working characteristics of the DMI strategy at high loads. During the GCI test, the injection pressure of the two injectors was set to 70 MPa, while that of the CDC mode was set to 120 MPa.

As a new methodology to improve the combustion deterioration of the GCI mode at high loads, suitably adjusting the energy ratio between the two main-injection is the key to achieving highly efficient and stable operation [15,25]. In addition, EGR is a regular method of the GCI mode at high loads, and the effect of EGR on this new strategy also needs to be investigated [26]. Therefore, to deeply study the combustion and emission characteristics of the DMI strategy, the effects of the energy ratio between the two main-injection and EGR were first tested at 10 bar IMEP. The specific experimental operating conditions are shown in Table 3. Afterward, high-load experiments were conducted using two injection strategies. The determination of the injection time at high loads was to achieve a higher thermal efficiency of the SMI strategy as much as possible while ensuring stable engine operation. Then, the injection time of the DMI strategy was kept the same as that of the SMI strategy, except that the injection time of the DMI strategy was delayed by 1 °CA compared to the SMI strategy at 15.5 bar IMEP because an earlier injection time of the DMI strategy would cause CA10 to occur before the top dead center. Although the injection time of the two strategies was different, the CA50 of the two operating points was close with an error of less than 0.3 °CA, which was still comparable [27]. In addition, the operating condition of the CDC test at high loads was similar to that in Ref. [28]. The operating conditions of the three modes at high loads are summarized in Table 4.

During the experiments, the engine speed was maintained at 1500 r/min (±2 r/min), while the oil temperature and the cooling water temperature were maintained at 85 °C (±2 °C) and 80°C (±2 °C), respectively. Since the experiments were performed at high loads, the fuel could be ignited stably without intake air heating. Therefore, the intake air temperature was kept at room temperature. The standard uncertainty in the experiment was comprehensively calculated by systematic uncertainties obtained by the experimental facilities and random uncertainties calculated by the function $\alpha = \sqrt{\frac{\sum_{i=1}^{n}(x_i - \bar{x})^2}{n-1}}$, where $x_i$ indicates the specific data in the experiment, $\bar{x}$, the

**Table 2** Properties of gasoline (G80) and No. 0 diesel

| Fuel | No. 0 diesel | G80 |
|---|---|---|
| RON | – | 82.7 |
| Cetane number | 52 | – |
| Density/($g \cdot cm^{-3}$) | 0.830 | 0.680–0.690 |
| Lower heating value/($MJ \cdot kg^{-1}$) | 42.7 | 44 |
| Initial boiling point/°C | 188 | 48–50 |
| 10% distillation temperature/°C | 214 | 59–62 |
| 50% distillation temperature/°C | 267 | 67–70 |
| 90% distillation temperature/°C | 353 | 80–83 |
| Final boiling point/°C | 360 | 98–101 |

**Table 3** Test conditions

| Parameter | Value |
|---|---|
| IMEP/bar | 10 |
| Intake pressure/bar | 1.75 |
| EGR/% | 0/30/40/45/55 |
| $SOI_1$ of Injector 1/(°CA ATDC) | −11 |
| Injection pressure 1/bar | 700 |
| $SOI_2$ of Injector 2/(°CA ATDC) | −11 |
| Injection pressure 2/bar | 700 |
| $R_{m\text{-}2}$/% | 0/7/19/32/42 |

**Note**: SOI–Start of injection.

**Table 4** Test conditions for SMI and DMI strategies

| Injection strategy | IMEP/bar | Intake pressure/bar | EGR/% | SOI/(°CA ATDC) | $R_{m\text{-}2}$/% |
|---|---|---|---|---|---|
| SMI/DMI | 12 | 2.1 | 45 | −11 | 0/10 |
| CDC | 12 | 1.3 | 15 | −7 | – |
| SMI/DMI | 14 | 2.4 | 40 | −11 | 0/10 |
| CDC | 14 | 1.45 | 22 | −7 | – |
| SMI | 15.5 | 2.5 | 37 | −13 | 0 |
| DMI | 15.5 | 2.5 | 37 | −12 | 10 |
| CDC | 15.5 | 1.65 | 30 | −7 | – |

average of the test data. The error bar was calculated by expanded uncertainty which was corresponding to the 95% confidence interval and twice of the standard uncertainty.

In this study, the carbon dioxide ($CO_2$) derived from the gas cylinder was added to the intake manifold to simulate the real EGR. The $EGR_{sim}$ was calculated as

$$\mathrm{EGR_{sim}}(\%) = \frac{\mathrm{CO}_{2\,\mathrm{intake}}\left(\times 10^{-6}\right)}{\mathrm{CO}_{2\,\mathrm{exhaust}}\left(\times 10^{-6}\right)} \times 100\%, \tag{1}$$

where $CO_{2\ intake}$ indicates the volume fraction of $CO_2$ in the intake manifold, while $CO_{2\ exhaust}$, the volume fraction of $CO_2$ in the exhaust manifold.

In the DMI strategy, the main-injection-2 ratio ($R_{m\text{-}2}$) is defined as the ratio of the energy of the main-injection-2 fuel to the energy of the total fuel, as indicated by

$$R_{\mathrm{m-2}} = \frac{m_2 \cdot \mathrm{LHV}_2}{m_1 \cdot \mathrm{LHV}_1 + m_2 \cdot \mathrm{LHV}_2}, \tag{2}$$

where $m_1$ and $m_2$ are the fuel mass flow rate of main-injection-1 and main-injection-2, respectively; $LHV_1$ and $LHV_2$ are the fuel low heating value (LHV) of main-injection-1 and main-injection-2, respectively.

To specifically reflect the influence of the DMI strategy on the in-cylinder fuel-gas mixing, the mean mixing time is defined in this paper to describe the overall fuel-gas mixing level [29]. The mean mixing time is calculated by

$$\text{Mean mixing time} = \frac{(\mathrm{CA10} - \mathrm{EOI}_1) * m_1 + (\mathrm{CA10} - \mathrm{EOI}_2) * m_2}{m_1 + m_2}, \tag{3}$$

where $EOI_1$ and $EOI_2$ represent the end of injection (EOI) of main-injection-1 and main-injection-2, respectively.

## 3 Results and discussion

### 3.1 Effect of $R_{m\text{-}2}$ on combustion and emission characteristics of DMI mode

By keeping the IMEP at 10 bar and the injection time of the two injectors at −11 °CA ATDC, the effect of the energy ratio between the two main-injection on combustion and emission characteristics of DMI mode were investigated. Figure 2 demonstrated the effect of the main-injection-2 ratio ($R_{m\text{-}2}$) on fuel-gas mixing time. As expected, the increase of $R_{m\text{-}2}$ resulted in a shorter injection duration for the engine cycle and an earlier end of injection (EOI). The mean mixing time defined in this paper could reflect the overall in-cylinder fuel-gas mixing quality to some extent. With the increase of $R_{m\text{-}2}$, the mean mixing time was prolonged, which meant that the fuel-gas mixing quality might be better.

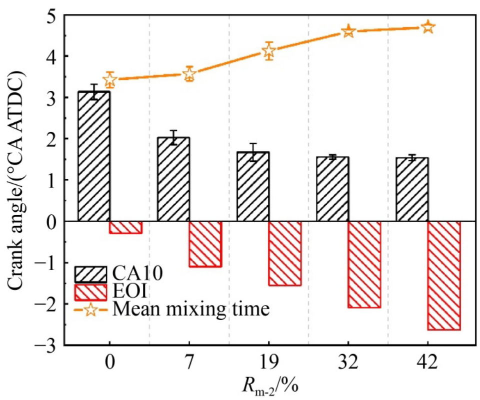


**Fig. 2** Effect of $R_{m\text{-}2}$ on fuel-gas mixing time.

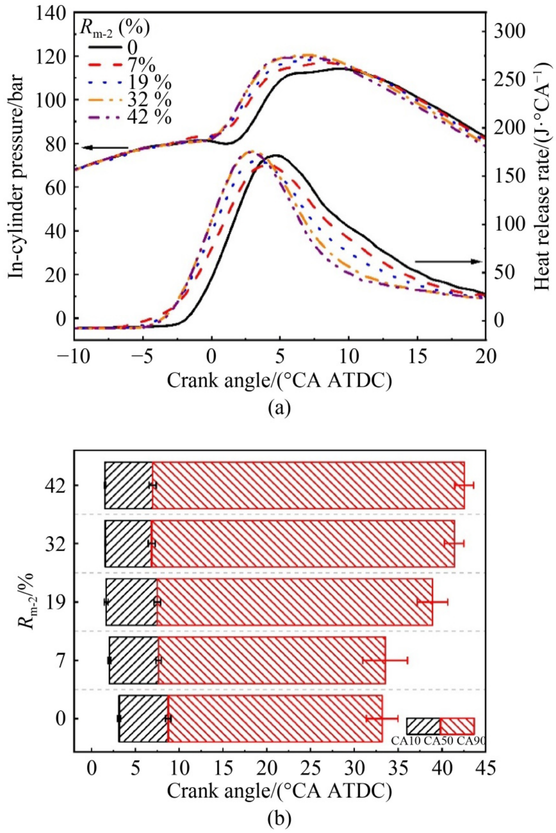


**Fig. 3** Effect of $R_{m\text{-}2}$ on (a) in-cylinder pressure, HRR, and (b) combustion phase.

Figure 3 exhibited the effect of $R_{m\text{-}2}$ on in-cylinder pressure, heat release rate (HRR), and combustion phase. As $R_{m\text{-}2}$ increased from 0 to 42%, CA10 and CA50 advanced and approached the top dead center (TDC), making the peak pressure increase. The simultaneous injection of the two injectors increased the in-cylinder charge reactivity, resulting in an earlier ignition timing of the fuel and more fuel burning near the TDC. Unlike CA10 and CA50, CA90 showed a tendency of delay. The HRR in the late stage of diffusion combustion was significantly reduced, which weakened the late oxidation rate of the remaining fuel and delayed the end point of heat release (CA90). In addition, more spray droplets attached to the piston and liner would delay CA90. The combination of CA10 advance and CA90 delay prolonged the combustion duration. Generally, the combustion process of the GCI mode could be divided into the low temperature reaction (LTR), the premixed combustion phase, and the mixing controlled combustion phase [15]. Thereinto, the maximum heat release rate ($HRR_{max}$) of premixed combustion was related to the degree of fuel premixing. Although the mean mixing time increased with the increase of $R_{m-2}$, $HRR_{max}$ decreased first and then increased. Considering the fact that the spray impinging between the two main-injection might increase the degree of in-cylinder fuel stratification, it was reasonable that $HRR_{max}$ decreased at first, indicating that the DMI strategy could shape the heat release to the desired pattern.

Figure 4 presented the effect of $R_{m-2}$ on regulated emissions (CO, THC, and $NO_x$) and combustion efficiency. As $R_{m-2}$ increased, the combustion phase approached the TDC, and a higher in-cylinder temperature and pressure accelerated the oxidation of incomplete emissions. Therefore, the combustion efficiency was extremely high with most cases above 99%. In particular, CO and THC emissions were less than 1 g/kWh and 0.4 g/kWh, respectively, when $R_{m-2}$ was between 7% and 19%. Compared with the previous results of port injection plus main injection with similar operating conditions, CO and THC emissions were reduced by about 90% and 80%, respectively [18]. However, when $R_{m-2}$ increased to 42%, a significant increase in CO and THC emissions happened due to the more fuel trapped in the crevice region, similar to the results obtained by increasing injection pressure [30]. The advanced combustion slightly increased $NO_x$ emissions due to the higher in-cylinder temperature.

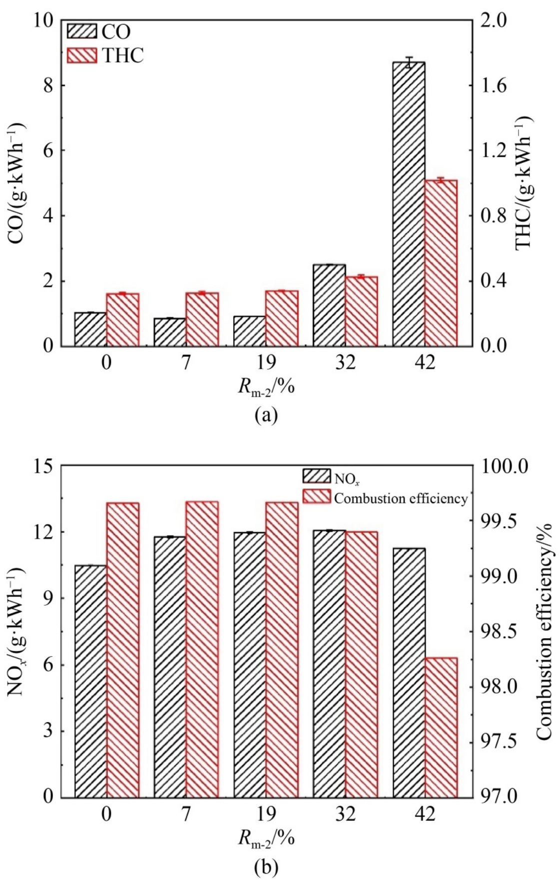


**Fig. 4** Effect of $R_{m-2}$ on regulated emission and combustion efficiency.

(a) CO and THC; (b) $NO_x$ and combustion efficiency.

Figure 5 depicted the effect of $R_{m-2}$ on unregulated emissions. According to the molecular structure, the unregulated emissions measured by FTIR are classified into saturated hydrocarbons, unsaturated hydrocarbons, and aldehydes. Saturated hydrocarbons such as methane, isopentane, and cyclohexane, and unsaturated hydrocarbons, such as ethylene and acetylene, are mainly derived from the cracking of big molecular organics and are consumed during the combustion process. When $R_{m-2}$ was less than 19%, the change in the energy ratio between the two main-injections had little effect on saturated and unsaturated hydrocarbons. However, when $R_{m-2}$ was raised to higher ratios (such as 32% and 42%), methane and unsaturated hydrocarbons significantly increased, similar to the result of THC emissions. Aldehydes (such as formaldehyde and acetaldehyde) are intermediate products of low temperature combustion,

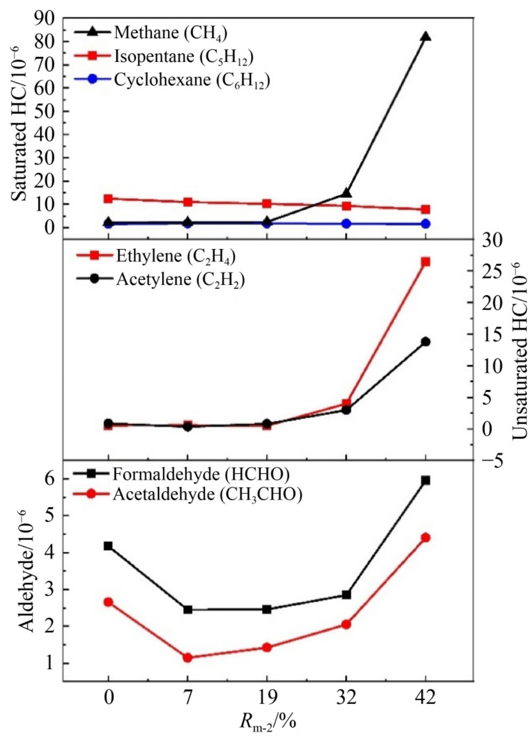


**Fig. 5** Effect of $R_{m-2}$ on unregulated emission.

and formaldehyde was usually regarded as the indicator of LTR in engine optical diagnosis [31]. Aldehydes mainly originated from the partial oxidation of unburned hydrocarbons in the cylinder and exhaust gas, thus aldehydes followed the same trend as THC emissions, such as the pattern of aldehydes in Fig. 5. It was worth noting that almost all unregulated emissions were close to zero when $R_{\text{m-2}}$ was 7% and 19%.

Particulate matter emissions can be divided into two types according to the particle size distributions. One is nucleation mode particle ($D_{\text{p}}$ < 50 nm) while the other is accumulation mode particle (50 nm < $D_{\text{p}}$ < 1000 nm). Toxicological studies suggested that animals exposed to ultrafine particles (below 100 nm) had a higher probability of coronary artery lesions than exposed to large particles, reducing ultrafine particles particularly important [32]. Figure 6 manifested the effect of $R_{\text{m-2}}$ on particle size distribution, particle number (PN), and geometric mean diameter (GMD). It was obviously observed that when $R_{\text{m-2}}$ increased from 0 to 19%, the number of nucleation mode particles decreased. Although the mean mixing time increased with the increase of $R_{\text{m-2}}$, more spray droplets from main-injection-2 adhered to the top of the piston and the cylinder liner due to the long spray penetration [33], increasing accumulation mode particles. Tuner et al. [34] also reported increased particulate emissions when using split injection for GCI test, and they believed that the higher level of soot was a consequence of too short a separation time for complete needle closure.

Figure 7 showed the relationship between maximum pressure rise rate (MPRR) and PN as well as indicated specific fuel consumption (ISFC). The closer the combustion phasing was to the TDC, the higher the MPRR and the less total particulate matter. As shown in Fig. 7(a), when $R_{\text{m-2}}$ was 7%, the DMI strategy had a comparable total particulate matter with the SMI strategy, while the DMI strategy resulted in a 1.4 bar/°CA reduction in MPRR. However, it was an unacceptable situation that the increase in mean mixing time led to an increase in MPRR along with an increase in PN due to more fuel adhering to the top of the piston and the cylinder liner. This phenomenon can be improved in the future by optimizing the position of injectors. In the lower MPRR and ISFC regions of Fig. 7(b), the MPRR and ISFC of the DMI strategy were lower than those of the SMI strategy when $R_{\text{m-2}}$ was 7% and 19%. Although the injection duration could be shortened by increasing the injection pressure to improve the fuel-gas mixing, increasing the injection pressure led to an over-mixing of the fuel,

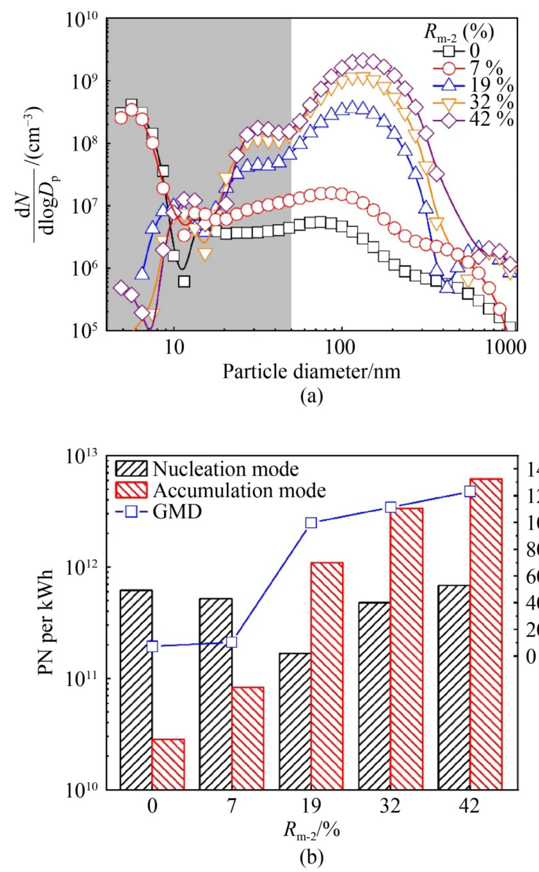


**Fig. 6** Effect of $R_{\text{m-2}}$ on (a) particle size distributions, (b) PN and GMD.

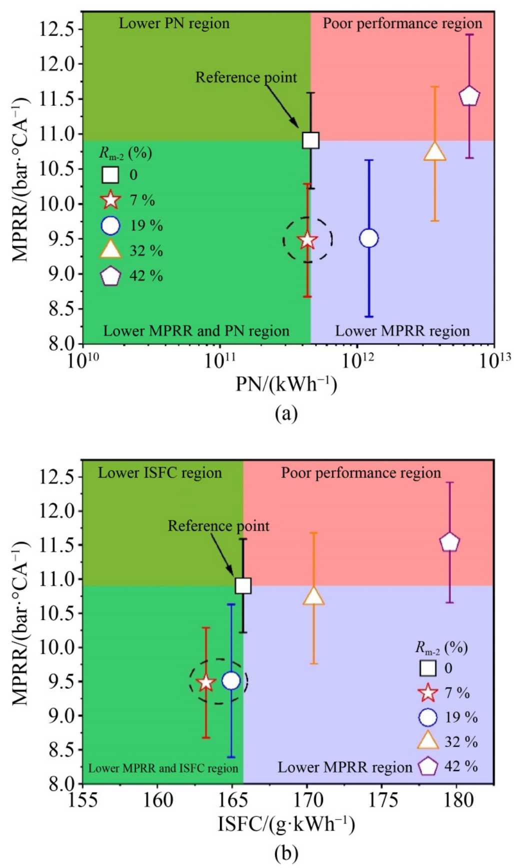


**Fig. 7** Correlations between (a) MPRR and PN, (b) MPRR and ISFC.

resulting in a higher MPRR [25,29]. The advantage of the DMI strategy was that it regulated concentration stratification and promoted fuel-gas mixing, thereby moderating the trade-off between MPRR and ISFC.

### 3.2 Effect of $EGR_{sim}$ on combustion and emission characteristics of DMI mode

For the typical GCI mode, the injection process and the combustion process were separated by adding an appropriate EGR to the cylinder to dilute the fuel-gas mixture, which delayed the combustion phase and reduced the MPRR [35]. In addition, EGR can reduce in-cylinder temperature and oxygen content to reduce $NO_x$ emissions. Therefore, it is necessary to investigate the influence of the EGR rate on combustion and emissions of the new injection strategy. In Section 3.1, the engine performed well with a good fuel economy, a proper fuel stratification, and low particulate emissions when $R_{m\text{-}2}$ was 7%. In Section 3.2, $EGR_{sim}$ varied from 0 to 55%, the injection timing of the two injectors was −11 °CA ATDC, $R_{m\text{-}2}$ was 7%, and IMEP was maintained at 10 bar. In addition, to reflect the effect of $EGR_{sim}$ on the DMI strategy, two operating conditions based on the SMI strategy with an $EGR_{sim}$ of 45% and without $EGR_{sim}$ were chosen for comparison.

Figure 8 plotted the effect of $EGR_{sim}$ on in-cylinder pressure and HRR. A higher $EGR_{sim}$ reduced the oxygen content and the air-fuel mixture reactivity, thereby delaying the phase of $HRR_{max}$. The retardation of the combustion phase increased the premixed combustion ratio, which made the combustion more concentrated and thus increased the $HRR_{max}$. There was no significant difference in the effect of $EGR_{sim}$ on in-cylinder pressure and HRR of these two strategies.

Figure 9 displayed the effect of $EGR_{sim}$ on ignition delay and combustion duration. The ignition delay and combustion duration are respectively calculated by

$$\text{Ignition Delay} = \text{CA10} - \text{SOI}, \tag{4}$$

$$\text{Combustion Duration} = \text{CA90} - \text{CA10}. \tag{5}$$

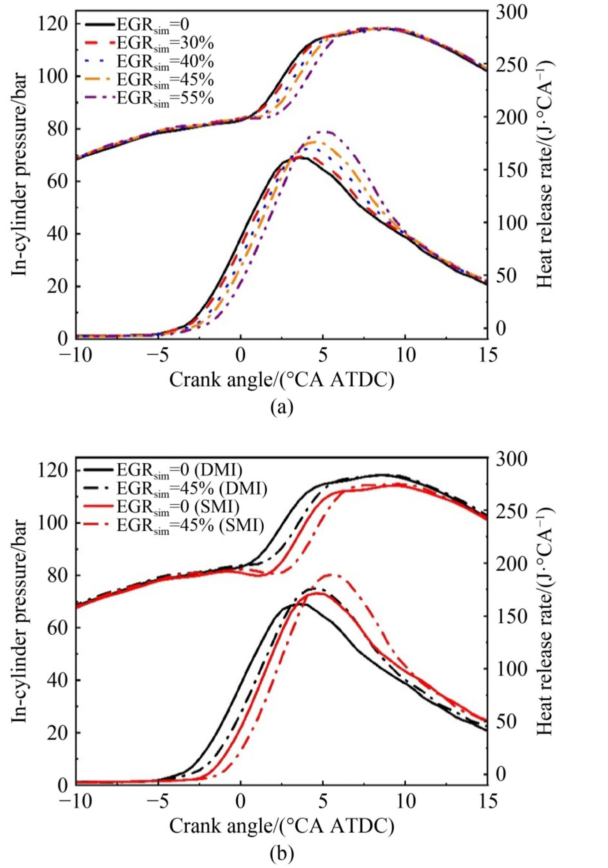


**Fig. 8** Effect of $EGR_{sim}$ on in-cylinder pressure and HRR of (a) DMI, (b) SMI strategies.

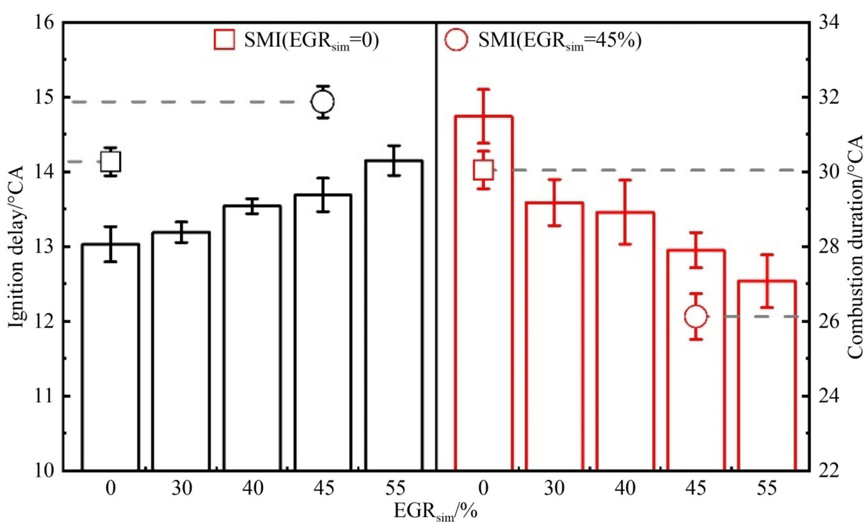


**Fig. 9** Effect of $EGR_{sim}$ on ignition delay and combustion duration.

With the increase in $EGR_{sim}$, the ignition delay of the low-octane gasoline was prolonged. The main reason for this was that $CO_2$ reduced the fuel-gas mixture reactivity in the cylinder, inducing a delay in the starting point of heat release, which was of great significance for the separation of injection and combustion of the new injection strategy. However, the longer ignition delay increased the premixed combustion ratio and made the heat release more concentrated and the combustion duration shortened. For the SMI strategy, the increase in $EGR_{sim}$ also shortened the combustion duration of the fuel.

Figure 10(a) showed the effect of $EGR_{sim}$ on CO and THC emissions. The increase in $EGR_{sim}$ would decrease the amount of oxygen and in-cylinder temperature, inhibiting the oxidation of CO emissions. However, the change in $EGR_{sim}$ had little effect on the in-cylinder temperature at high loads. Therefore, it can be assumed that the increase in CO emissions was mainly caused by the reduction of oxygen content [36]. THC emissions mainly originated from three sources: incomplete combustion, unburned hydrocarbons in the boundary layer, and the cylinder wall quenching effect [37]. The results in Fig. 10(a) suggested that $EGR_{sim}$ had little effect on THC emissions of the DMI strategy. $EGR_{sim}$ had a more pronounced effect on CO and THC emissions of the SMI strategy with a larger increment. In addition, the CO and THC emissions were at low levels, which indicated that the DMI strategy could obtain an ultrahigh combustion efficiency even at large EGR rates.

Figure 10(b) showed the effect of $EGR_{sim}$ on particle size distribution. At low-to-medium loads, the increase in $EGR_{sim}$ would prolong the fuel-gas mixing time, which reduced the local rich zone in the cylinder and thus effectively reduced the particulate matter. At medium-to-high loads, although $EGR_{sim}$ would increase the fuel-gas mixing time, the reduction of oxygen content would be detrimental to the oxidation of particulate matter [17]. In this experiment, the increase in $EGR_{sim}$ reduced the nucleation mode particles while having a less pronounced effect on accumulation mode particles. The results in Fig. 11 indicated that $EGR_{sim}$ had less impact on unregulated emissions, because most of the unregulated emissions were no more than $5 \times 10^{-6}$ except for isopentane.

Figure 12(a) showed the relationship between PN and MPRR, in which, it could be observed that there was an obvious trade-off between PN and MPRR. With the increase in $EGR_{sim}$, the total number of particles decreased and MPRR increased, also for the SMI strategy. In Fig. 9, the SMI strategy without $EGR_{sim}$ and the DMI strategy with an $EGR_{sim}$ of 55% had the same injection time with similar ignition delays. However, the DMI strategy had a lower MPRR and PN even with an $EGR_{sim}$ of 55%, which again demonstrated that the DMI strategy

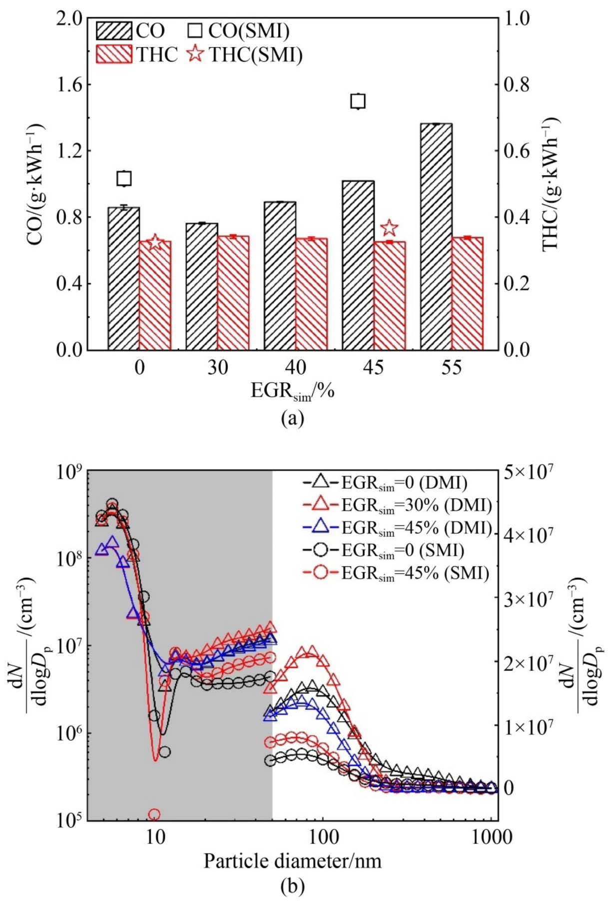


**Fig. 10** Effect of $EGR_{sim}$ on (a) CO, THC, and (b) particulate matter emissions.

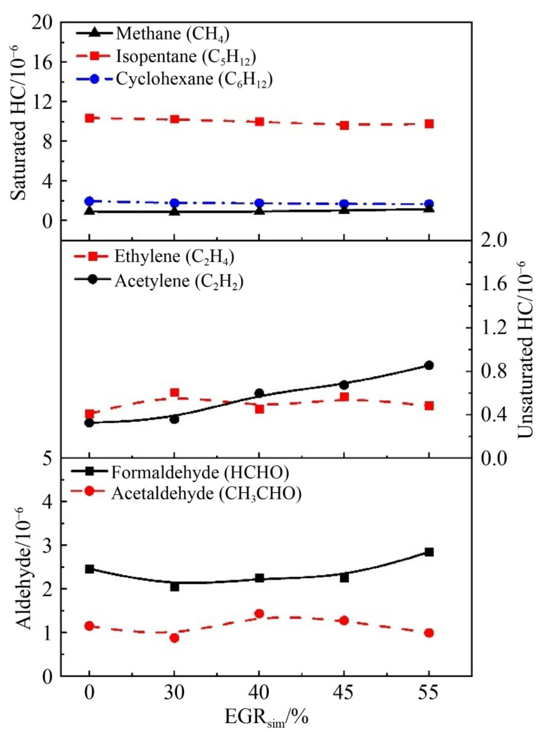


**Fig. 11** Effect of $EGR_{sim}$ on unregulated emissions.

could regulate in-cylinder fuel stratification and promote fuel-gas mixing. In addition, $EGR_{sim}$ had a more significant effect on reducing the PN of the DMI strategy.

In Fig. 12(b), $NO_x$ emissions were reduced to about 6 g/kWh with an ITE of around 49% when $EGR_{sim}$ was 55%. Compared to the SMI strategy with an $EGR_{sim}$ of 45%, both the SMI strategy and the DMI strategy had similar $NO_x$ emissions, but the DMI strategy had a higher thermal efficiency and a lower PN. It can also be seen from Fig. 12(b) that with the increase in $EGR_{sim}$, both $NO_x$ emissions and ITE decreased. $EGR_{sim}$ would reduce the oxygen concentration in the cylinder, which reduced the contact between oxygen and fuel as well as nitrogen, thus inhibiting the whole oxidation process in the cylinder. Although the cold EGR had a high specific heat capacity and could reduce the combustion temperature of the cycle, the thermodynamic effect of the cold EGR had little impact at high loads. This conclusion could be drawn from the results of Zeraati-Rezaei et al. [26] using the hot EGR to reduce $NO_x$ emissions, and they believed that the dilution effect of EGR would be more pronounced. This experiment demonstrated that EGR could reduce $NO_x$ and particulate matter emissions of G80, but increase MPRR and decrease ITE. Therefore, a proper EGR rate should be adopted considering the trade-off between combustion and emissions.

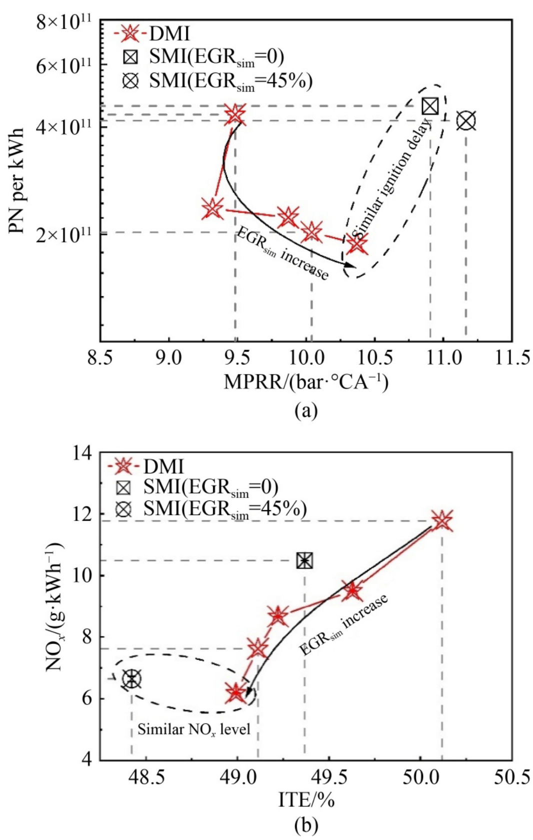

**Fig. 12** Correlations between (a) MPRR and PN as well as (b) ITE and $NO_x$.

### 3.3 Comparison of combustion and emissions of DMI mode and SMI mode at high loads

Based on Sections 3.1 and 3.2, it can be concluded that reasonably adjusting the energy ratio between the two main-injection could achieve an appropriate fuel stratification and a better fuel-gas mixing. In Section 3, experiments were conducted using the DMI strategy under higher engine load conditions and compared to the SMI and the CDC modes.

Figure 13 showed the in-cylinder pressure and HRR of G80 based on the two injection strategies. With the increase of engine load, the injection duration was prolonged, the fuel-gas mixing time was shortened, the main $HRR_{max}$ decreased, and the HRR profile showed a clear bimodal exothermic shape. The HRR profile of the SMI strategy was similar, which indicated that both strategies showed a vast proportion of mixing controlled combustion. If continuing increasing the engine load, the combustion characteristic would be more similar to diesel combustion.

Under higher load conditions, the DMI strategy still reduced the peak heat release of premixed combustion due to the fuel regulation effect. Different from the single-injector multi-stage injection strategy, the LTR

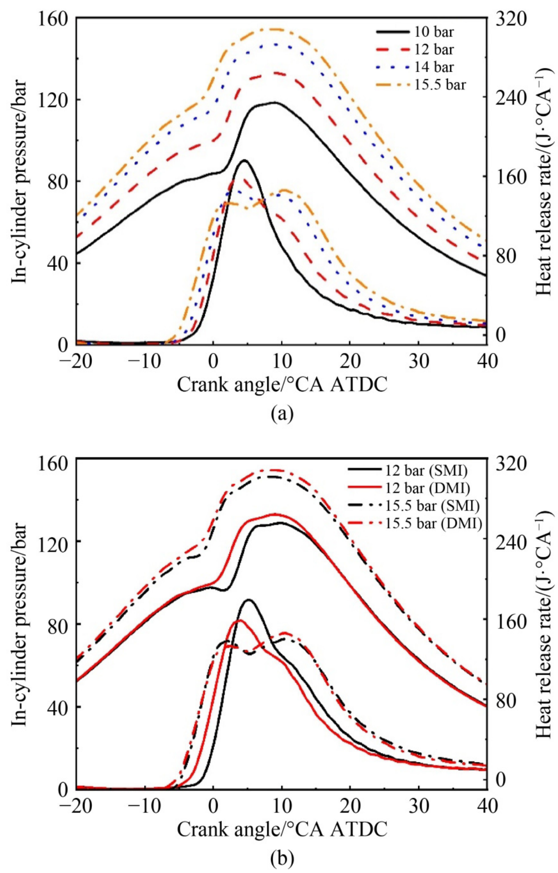

**Fig. 13** In-cylinder pressure and HRR for (a) DMI; (b) SMI strategies at high loads.

phenomenon did not occur for the two injection strategies. The reason for this was that the injection timing of the two strategies was close to the TDC when the in-cylinder temperature had exceeded the suitable temperature range for the cool flame reaction, which was related to the LTR phenomenon [38].

Figure 14 compared the regulated emissions, including CO, $NO_x$, and THC emissions, for the two injection strategies. In addition, the relevant emissions of the prototype diesel combustion were also plotted for comparison. At high loads, both CO and THC emissions were low (below 1 g/kWh) due to the extremely high in-cylinder temperature and pressure. The CO and THC emissions of the DMI strategy were less or comparable with those of the SMI strategy. As the load increased, the DMI mode had lower CO and THC emissions than the CDC mode. In addition, the DMI strategy would slightly increase $NO_x$ emissions due to the higher in-cylinder temperature, but this phenomenon weakened at a higher load. The more concentrated combustion and the combustion phase closer to the top dead center resulted in a higher $NO_x$ emission in the GCI mode than in the CDC mode. The high-load experiment was conducted on the principle of thermal efficiency priority, and $NO_x$ emissions did not drop below 5 g/kWh. Some studies showed that the injection timing had a significant effect on $NO_x$ emissions [3]. Further study can be conducted to explore the influence of injection timing on combustion and emissions of the DMI mode.

Figure 15 displayed the unregulated emissions of G80 of the two injection strategies. As the load increased, most of the unregulated emissions decreased due to the high degree of complete combustion, and some emissions were even less than $1 \times 10^{-6}$, such as unsaturated hydrocarbons and methane. Among the saturated hydrocarbons, the amount of isopentane was significantly higher than that of methane, and the relationship of isopentane between the two strategies was the same as that of THC emissions. The aldehydes of the DMI strategy were less than those of the SMI strategy.

Figure 16 showed comparisons of PM and PN (a) ITE and MPRR (b) of different modes at high loads. Of the three modes, the DMI mode had the highest PN emission, while the PM emission of the DMI mode was the lowest, which indicated that the particulate matter in the DMI mode was mainly in the nucleation mode. As the load increased, the PM emission of the CDC mode increased significantly while the increment of PM emission was smaller in the GCI mode, which indirectly indicated the potential of the GCI mode to improve PM emission at high loads.

Wei et al. [39] indicated that the knock phenomenon of the GCI mode was caused by the rapid combustion of the mixture in multiple places with a large MPRR and $HRR_{max}$. This paper set the stable value of MPRR of DMI mode to 10 bar/°CA. At high loads, the MPRR of all cases with the DMI strategy was smaller than that of the SMI strategy, and the ITE of the DMI strategy was improved. Specifically, when the IMEP was 15.5 bar with a similar CA50 of the two strategies, the MPRR of the DMI mode was reduced by about 1.5 bar/°CA, and the ITE of the DMI mode was increased by about 0.7%. Li et al. [22] also performed high load tests in the GCI mode adopting the port injection in combination with the direct injection strategy, with a load range from 12 bar to 13 bar. However, the ITE of this strategy was below 45% at high loads. In this paper, all high-load cases with the DMI strategy were in high efficiency regions with an ITE greater than 48%. The MPRR of the CDC mode was significantly lower than that of the GCI mode due to the

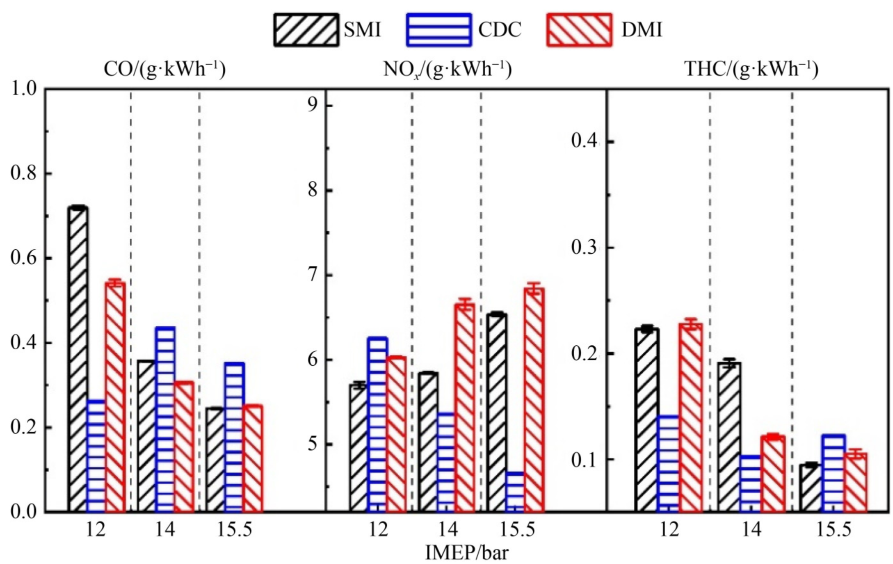


**Fig. 14** Comparison of regulated emissions for different injection strategies at high loads.

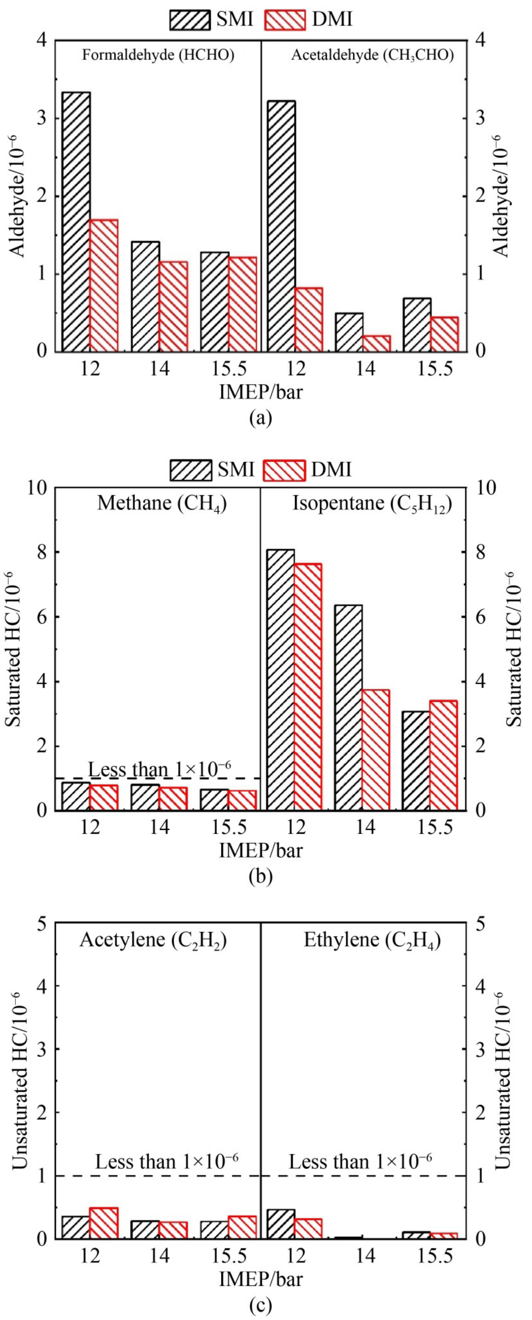


**Fig. 15** Comparison of unregulated emissions for different injection strategies at high loads.

(a) Aldehyde; (b) saturated HCs; (c) unsaturated HCs.

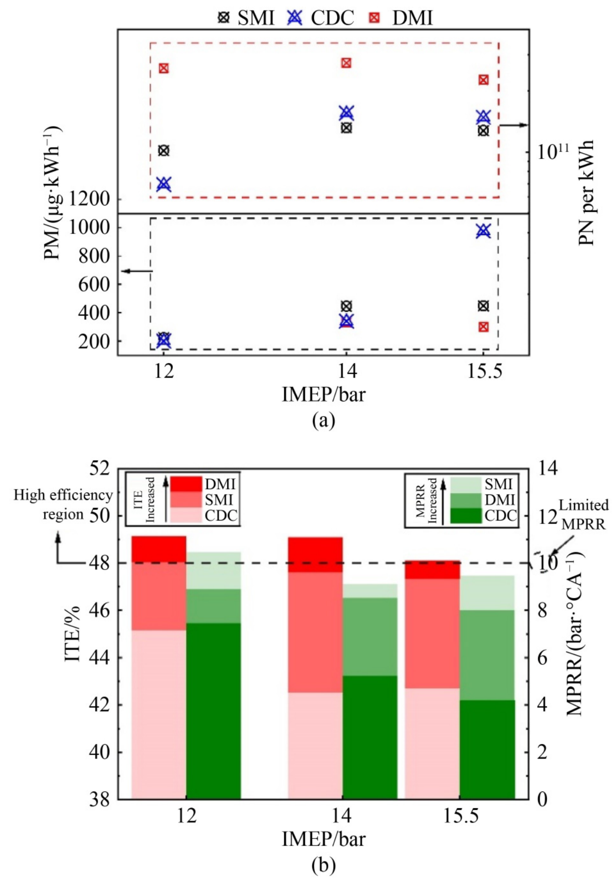


**Fig. 16** Comparisons of (a) PM and PN; (b) ITE and MPRR for different injection strategies at high loads.

large proportion of diffusion combustion. At high loads, the GCI mode had a better fuel-gas mixing state than the CDC mode. As a result, the ITE of the GCI mode was significantly higher than that of the CDC mode. The results of Mao et al. [40] showed that the low viscosity of the fuel had an adverse effect on their injection pressure and fuel economy at high loads. Significantly, the double main-injection strategy not only alleviated the requirement of the GCI mode on the fuel injection pressure but also achieved a higher thermal efficiency with a lower MPRR, which was of great significance to improving the problem of combustion deterioration at high loads in the GCI mode.

## 4 Conclusions

In this paper, two direct injectors were used for the simultaneously main-injection, called the double main-injection (DMI) strategy, to improve the problems of high maximum pressure rise rate (MPRR) and combustion deterioration of the GCI mode at high loads. The effects of the energy ratio of the main-injection-2 ($R_{m\text{-}2}$) and EGR on combustion and emissions were investigated. The DMI strategy was used to conduct high-load experiments and compared with the single main-injection (SMI) strategy and conventional diesel combustion (CDC). The main findings can be summarized as follows:

1) In the DMI mode, the simultaneous main-injection of the two direct injectors can achieve a rapid fuel supply and control of fuel stratification. When $R_{m\text{-}2}$ increases, the mean mixing time increases, and MPRR and indicated specific fuel consumption decreases first and then increases. A large amount of main-injection-2 causes the fuel to adhere to the piston top and cylinder liner,

resulting in a deterioration of combustion and emissions.

2) EGR has a significant effect on the combustion and emissions of the DMI mode. When the EGR rate increases from 0 to 55%, $NO_x$ emissions are reduced by about 6 g/kWh. EGR will delay the combustion phase and thus reduce ITE. The increase in the EGR rate decreases the particulate number while increasing the MPRR. Therefore, a proper EGR rate should be adopted considering combustion and emissions.

3) The DMI strategy achieves a highly efficient and stable combustion of the GCI mode. At high loads, the ITE is greater than 48%, the CO and THC emissions are at low levels (below $1 \times 10^{-4}$), and the MPRR is within a reasonable range. With the increase of engine load, the diffusion combustion ratio increases, and the heat release rate profile has a bimodal exothermic shape.

4) The DMI strategy can alleviate the requirement of the GCI mode on injection pressure and improve the problems of high MPRR and combustion deterioration. Compared with the SMI strategy at high loads, the DMI strategy exhibits a higher ITE and a lower MPRR. At 15.5 bar, the MPRR reduces by about 1.5 bar/°CA, and the ITE increases by about 0.7%. The CO and THC emissions of the DMI mode are less or comparable with those of the SMI mode. The main drawback of the DMI mode is that it slightly increases $NO_x$ emissions.

The DMI strategy can improve the fuel economy and reduce MPRR at high loads, which is significant for the GCI mode. However, this is only a preliminary attempt at the two direct injectors of the engine in the GCI mode. In the future, the effect of injection time can be investigated to achieve clean combustion. Moreover, the CFD simulation to optimize the injection position of the injectors seems necessary.

**Acknowledgment** This work was supported by the National Key R&D Program of China (Grant No. 2022YFE0100100).

**Competing interests** The authors declare that they have no competing interests.

## References

1. Zhao T, Ren Z, Yang K, et al. Combustion and emissions of RP-3 jet fuel and diesel fuel in a single-cylinder diesel engine. Frontiers in Energy, 2021, online, https://doi.org/10.1007/s11708-021-0787-3
2. Xia C, Zhao T, Fang J, et al. Experimental study of stratified lean burn characteristics on a dual injection gasoline engine. Frontiers in Energy, 2022, online, https://doi.org/10.1007/s11708-021-0812-6
3. Kalghatgi G T, Ångström H E. Advantages of fuels with high resistance to auto-ignition in late-injection, low-temperature, compression ignition combustion. SAE Technical Papers: 2006–01–3385, 2006
4. Dec J E. Advanced compression-ignition engines–understanding the in-cylinder processes. Proceedings of the Combustion Institute, 2009, 32(2): 2727–2742
5. Zhang P, Xu G, Li Y, et al. Collaborative optimization of fuel composition and operating parameters of gasoline compression ignition (GCI) engine in a wide load range. Fuel, 2022, 310: 122366
6. Wang H, Zhu H, Ma T, et al. Numerical investigation on low octane gasoline-like fuel compression ignition combustion at high load. Fuel, 2020, 270: 117532
7. Hanson R, Splitter D, Reitz R. Operating a heavy-duty direct-injection compression-ignition engine with gasoline for low emissions. SAE Technical Paper: 2009–01–1442, 2009
8. Kim K, Kim D, Jung Y, et al. Spray and combustion characteristics of gasoline and diesel in a direct injection compression ignition engine. Fuel, 2013, 109: 616–626
9. Ciatti S, Subramanian S N. An experimental investigation of low-octane gasoline in diesel engines. Journal of Engineering for Gas Turbines and Power, 2011, 133(9): 092802
10. Kalghatgi G T, Kumara Gurubaran R, Davenport A, et al. Some advantages and challenges of running a Euro IV, V6 diesel engine on a gasoline fuel. Fuel, 2013, 108: 197–207
11. Sellnau M, Foster M, Moore W, et al. Pathway to 50% brake thermal efficiency using gasoline direct injection compression ignition. SAE International Journal of Advances and Current Practices in Mobility, 2019, 1(4): 1581–1603
12. Pan J, Li X, Yin Z, et al. Effects of intake conditions and octane sensitivity on GCI combustion at early injection timings. Fuel, 2021, 298(5): 120803
13. An Y, Raman V, Tang Q, et al. Combustion stability study of partially premixed combustion with low-octane fuel at low engine load conditions. Applied Energy, 2019, 235: 56–67
14. Torelli R, Pei Y, Zhang Y, et al. Effect of fuel temperature on the performance of a heavy-duty diesel injector operating with gasoline. SAE Technical Paper: 2021–01–0547, 2021
15. Liu H, Mao B, Liu J, et al. Pilot injection strategy management of gasoline compression ignition (GCI) combustion in a multi-cylinder diesel engine. Fuel, 2018, 221: 116–127
16. Leermakers C A J, Bakker P C, Nijssen B C W, et al. Low octane fuel composition effects on the load range capability of partially premixed combustion. Fuel, 2014, 135: 210–222
17. Bobi S, Kashif M, Laoonual Y. Combustion and emission control strategies for partially-premixed charge compression ignition engines: a review. Fuel, 2022, 310: 122272
18. Jiang C X, Li Z L, Qian Y, et al. Towards low emissions and high thermal efficiency of gasoline compression ignition engine under high loads by modulating the fuel reactivity and injection strategy. Science China. Technological Sciences, 2020, 63(1): 96–104
19. Xia J, Zhang Q, He Z, et al. Experimental study on diesel’s twin injection and spray impingement characteristics under marine engine’s conditions. Fuel, 2021, 302: 121133
20. Avulapati M M, Rayavarapu Venkata R. Experimental studies on air-assisted impinging jet atomization. International Journal of Multiphase Flow, 2013, 57: 88–101
21. Noce T, de Morais Hanriot S, Sales L C M, et al. Energy conversion factor for gasoline engines in real-world driving

emission cycle. Automotive Innovation, 2020, 3(2): 169–180

22. Li Z, Xia J, Jiang C, et al. Experimental study on wide load operation of gasoline compression ignition engine: real distillate gasoline versus primary reference fuel. Fuel, 2020, 277: 118211
23. Kalghatgi G, Hildingsson L, Johansson B. Low $NO_x$ and low smoke operation of a diesel engine using gasolinelike fuels. Journal of Engineering for Gas Turbines and Power, 2010, 132(9): 092803
24. Hao H, Liu F, Liu Z, et al. Compression ignition of low-octane gasoline: life cycle energy consumption and greenhouse gas emissions. Applied Energy, 2016, 181: 391–398
25. Liu J, Wang H, Zheng Z, et al. Improvement of high load performance in gasoline compression ignition engine with PODE and multiple-injection strategy. Fuel, 2018, 234: 1459–1468
26. Zeraati-Rezaei S, Al-Qahtani Y, Xu H. Investigation of hot-EGR and low pressure injection strategy for a dieseline fuelled PCI engine. Fuel, 2017, 207: 165–178
27. Manente V, Johansson B, Tunestal P. Characterization of partially premixed combustion with ethanol: EGR sweeps, low and maximum loads. Journal of Engineering for Gas Turbines and Power, 2010, 132(8): 082802
28. Zhang Y, Wu H, Mi S, et al. Application of methanol and optimization of mixture design over the full operating map in an intelligent charge compression ignition (ICCI) engine. Fuel Processing Technology, 2022, 234: 107345
29. Zou X, Liu W, Lin Z, et al. An experimental investigation of the effects of fuel injection strategy on the efficiency and emissions of a heavy-duty engine at high load with gasoline compression ignition. Fuel, 2018, 220: 437–445
30. Coratella C, Parry L, Li Y, et al. Experimental investigation of the rail pressure fluctuations correlated with fuel properties and injection settings. Automotive Innovation, 2021, 4(2): 215–226
31. Tang Q, Liu H, Li M, et al. Optical study of spray-wall impingement impact on early-injection gasoline partially premixed combustion at low engine load. Applied Energy, 2017, 185: 708–719
32. Li N, Sioutas C, Cho A, et al. Ultrafine particulate pollutants induce oxidative stress and mitochondrial damage. Environmental Health Perspectives, 2003, 111(4): 455–460
33. Liu H, Ma S, Zhang Z, et al. Study of the control strategies on soot reduction under early-injection conditions on a diesel engine. Fuel, 2015, 139: 472–481
34. Tuner M, Johansson T, Aulin H, et al. Multi cylinder partially premixed combustion performance using commercial light-duty engine hardware. SAE Technical Paper: 2014–01–2680, 2014
35. Shen M, Tuner M, Johansson B, et al. Effects of EGR and intake pressure on PPC of conventional diesel, gasoline and ethanol in a heavy duty diesel engine. SAE Technical Paper: 2013–01–2702, 2013
36. He T, Chen Z, Zhu L, et al. The influence of alcohol additives and EGR on the combustion and emission characteristics of diesel engine under high-load condition. Applied Thermal Engineering, 2018, 140: 363–372
37. Jiang C, Huang G, Liu G, et al. Optimizing gasoline compression ignition engine performance and emissions: combined effects of exhaust gas recirculation and fuel octane number. Applied Thermal Engineering, 2019, 153: 669–677
38. Wei H, Liu F, Pan J, et al. Experimental study on the effect of pre-ignition heat release on GCI engine combustion. Fuel, 2020, 262: 116562
39. Wei H, Yu J, Zhou L. Improvement of engine performance with high compression ratio based on knock suppression using Miller cycle with boost pressure and split injection. Frontiers in Energy, 2019, 13(4): 691–706
40. Mao B, Liu H, Zheng Z, et al. Influence of fuel properties on multi-cylinder PPC operation over a wide range of EGR and operating conditions. Fuel, 2018, 215: 352–362